波長分散型蛍光X線分析装置を用いた黒曜石の化学分析-考古学的石器石材の非破壊化学分析法の開発-

資源環境と人類　第2号　1-14頁　2012年3月
Natural Resource Environment and Humans
No.2. March 2012. pp. 1-14.

Chemical analysis of obsidian by Wave length-dispersive X-ray fluorescence spectrometry: application to nondestructive analysis of archeological obsidian artifacts

Yoshimitsu Suda*

Abstract

Wave length-dispersive X-ray fluorescence (WDXRF) spectrometry was installed at Meiji University Center for Obsidian and Lithic Studies. The XRF determines the abundances of element in a material, which has been applied to the chemical analysis of archeological obsidian artifacts in order to identify a place of their sources. The WDXRF is suited to perform an accurate chemical analysis of obsidian. For the characterization of obsidian in Nagawa town area (Takayama, Omegura, and Wada touge), quantitative analysis of the obsidian by fused glass bead method was performed, and a way of nondestructive analysis for the archeological obsidian artifacts was examined. Results of quantitative analysis indicate that variation of Sr/Rb ratio and Y/Sr ratio becomes good indicator to characterize the geochemistry of obsidian, which can be theoretically explained by the fractional crystallization process of feldspars. Results of analysis using the polished, flaked and weathered surfaces of obsidian indicate that the peak-over-background method, and the way of data expression normalized to the value after a standard sample were effective to link them with the results of quantitative analysis. In this study, the polished surface of obsidian from Shirataki in Hokkaido (obstd-1) was used as the standard sample. Namely, this study suggests that the ways of analysis and evaluation using the standard sample and values, such as the obstd-1, is quite useful on the nondestructive analysis, which can directly be applied to the analysis of archeological obsidian artifacts.

Key words: obsidian, X-ray fluorescence spectrometry, chemical analysis, geochemistry, Nagawa town.

Introduction

Continental crust is characterized by the occurrence of felsic magma. In most of the cases, obsidian is formed during eruption of such the felsic magma. Thus, the obsidian is quite informative to reveal an evolution of continental crust in earth history. From another point of view, the human has been used the obsidian as resources for making an artifact tool, and the industrial products, such as paved material and filtering material. Thus, it could be said that the obsidian has been closely related with a human life or living from ancient to present. For instance, a trace of archeological obsidian from acquirement to consumption becomes a good indicator to reveal human behavior during ancient times. Kuzmin (2011) indicates that distribution of the Paleolithic obsidian artifacts made of Shirataki obsidian in Hokkaido, is extended to the Sakhalin Island.

The geologist will use a chemical data for the characterization of a sample on the basis of physicochemical and kinetic theories (e.g. geochemical modeling). On the other hand, the archeologist will use a chemical data for discrimination or identification on the basis of experience and/or statistic theory. Consequently, it could be said that the aim to perform a chemical analysis of obsidian is quite differed between the archeological research work, and the geological research work, although the same analytical appliances, such as X-ray fluorescence (XRF) spectrometry, Laser ablation inductively coupled plasma mass spectrometry (LA-ICP-MS), Instrumental neutron activation analysis (INAA), and Particle induced X-ray emission (PIXE), are used in both research works. In the geological research work, a chemical data is commonly expressed by an absolute value of mass percentage, such as weight percent (wt.%) and parts per million (ppm). The major elements are expressed by oxides using the wt.% (SiO_2, TiO_2, and Al_2O_3 wt.% etc.), which are able to check whether or not the total amount becomes ca. 100 wt.%. On the other hand, in the archeological research work, the chemical data is generally expressed by fraction

* Meiji University Center for Obsidian and Lithic Studies
geosuda@gmail.com

of elements (%), and X-ray intensity, (counts or count per second), of a specific spectrum or line obtained from the XRF analysis. This way of data expression is enough for the discrimination of obsidian. In fact, Mochizuki *et al.* (1994) proposed the very effective way of discrimination diagram of obsidian using the X-ray intensity, and Ikeya (2009) demonstrated the usage of this way of discrimination on his archeological research work. However, the problem still remaining is the results obtained from this way cannot be shared and verified among researchers.

The X-ray intensity of spectrum or line for a specific element is roughly correlated with the abundance of the element. However, precisely speaking, in order to link the X-ray intensity with the actual abundances of elements in a sample, the calculations to correct the absorption and excitation effects by matrix elements (i.e. matrix effect), and overlap spectrum on an analyzed spectrum or line are necessary. Moreover, the way of data expression by an absolute value (i.e. wt.% and ppm) is necessary to be shared and verified among researchers and research laboratories.

There are two major purposes in this study. One is how the method of geological or petrological analysis can be applied to the archeological research work. Second is how we should present the data of nondestructive analysis to be shared among researchers. In this study, focusing on the analysis using the Wave length-dispersive X-ray fluorescence (WDXRF) spectrometry, the way of quantitative analysis by fused glass bead method is established. Then, the geochemistry of obsidians in the Nagawa town area (Takayama, Omegura and Wada touge) is characterized. Finally, a way of nondestructive analysis for the archeological obsidian artifacts is examined.

1. X-ray fluorescence (XRF) spectrometer

The XRF analysis determines the abundance of elements in a material, which has been used for the chemical analyses of rocks, minerals, sediments, soils, steels, and water. Chemical analysis of obsidian artifacts using the XRF has been commonly performed in the archeological research work, where the purpose of analysis is generally focused on the identification for the source of obsidian artifacts (e.g. Shackley 2011). In order to establish a chemical analysis system for the archeological and geological obsidians, three types of the XRFs: WDXRF (Rigaku ZSX PrimusIII+), Energy-dispersive X-ray spectroscopy (EDXRF: JEOL JSX-3100II), and Handheld or Portable X-ray spectroscopy (PXRF: Innov-X Delta Premium), was recently installed at Center for Obsidian and Lithic Studies (COLS). Among these XRFs, the WDXRF is the largest in size, which is equipped with the highest power X-ray anode (3kW Rh anode X-ray tube). The WDXRF is capable of dividing the X-ray photons according to a specific

Table 1. Instrumental conditions for quantitative analysis

Application name:			RockWS3.2				Diaphragm:		30 mm							
Sample:			110ºC base				Flux:		Merk Spectromelt A12							
Spin:			On				Standard:		GSJ Igneous (22) + sedimentary (1)							
Matrix correction:			de Jongh model				Dilution rate:		2.065 (flux 3.6000g + sample 1.8000g + $LiNO_3$ 0.54g)							
									Count time (s)				Angle (deg)			
	Line		Target	kV	mA	Filter	Slit	Crystal	Detector	Peak	BG1	BG2	total	Peak	BG1	BG2
14	Si	Kα	Rh	50	50	out	S4	PET	PC	60	-	-	60	109.030	-	-
22	Ti	Kα	Rh	50	50	out	S2	LiF(200)	SC	40	20	20	80	86.110	84.820	87.886
13	Al	Kα	Rh	50	50	out	S4	PET	PC	40	20	20	80	144.770	140.650	147.970
26	Fe	Kα	Rh	50	50	out	S2	LiF(200)	SC	40	40	-	80	57.494	55.476	-
25	Mn	Kα	Rh	50	50	out	S2	LiF(200)	SC	40	20	20	80	62.950	62.058	64.020
12	Mg	Kα	Rh	50	50	out	S4	RX25	PC	40	20	20	80	37.984	34.210	40.110
20	Ca	Kα	Rh	50	50	out	S4	LiF(200)	PC	40	20	20	80	113.124	110.160	-
11	Na	Kα	Rh	50	50	out	S4	RX25	PC	40	20	20	80	46.130	43.440	48.380
19	K	Kα	Rh	50	50	out	S4	LiF(200)	PC	40	20	20	80	136.674	133.350	139.940
15	P	Kα	Rh	50	50	out	S4	Ge	PC	40	20	20	80	141.050	137.912	143.230
37	Rb	Kα	Rh	50	50	out	S2	LiF(220)	SC	120	60	60	240	37.948	37.546	38.458
38	Sr	Kα	Rh	50	50	out	S2	LiF(200)	SC	100	50	50	200	25.134	24.706	25.540
39	Y	Kα	Rh	50	50	out	S2	LiF(200)	SC	100	50	50	200	23.740	23.382	24.258
40	Zr	Kα	Rh	50	50	out	S2	LiF(220)	SC	120	60	60	240	32.048	31.606	32.812
												total	27.7	min		

energy or wavelength by a higher resolution. Therefore, the WDXRF is best suited to carry out a quantitative analysis by accuracy of a high degree. On the other hand, the EDXRF and PXRF are equipped with the 50W Rh anode X-ray tube, and 0.5W Rh anode X-ray tube, respectively. Although resolution of spectrum is inferior to those of the WDXRF, the smaller size of these instruments helps to handle them easily. The EDXRF can be used on a working desk. The PXRF can be used at anywhere from a laboratory to a field. Furthermore, the sample size is limited to less than 5.0cm in the case of WDXRF analysis, whereas the sample size can be several tens of centimeters size in the case of EDXRF analysis, and there is no limitation in sample size in the case of PXRF analysis. The analytical appliance can be chosen on the basis of sample size and/or requirement of analytical accuracy and precision.

2. Quantitative analysis by fused glass bead method

2-1 Instrumental conditions

Calibration lines for the analysis elements were constructed using the following geochemical reference samples from Geological Society of Japan (GSJ: JA-1, JA-2, JA-3, JB-1, JB-2, JB-3, JR-1, JR-2, JR-3, JG-1a, JG-2, JGb-1, JGb-2, JP-1, JF-1, JF-2, JH-1, JSy-1). The H_2O- (absorbed water) in a sample was released by heating at 110°C for more than 6 hour. Low dilution fused glass bead for the analysis was prepared by the following manner: a sample powder (1.6000 g) was mixed with a flux (Merck Spectromelt A12: 3.6000 g) and an oxidizing reagent (Wako HNO_3: 0.54 g), and kept in a platinum crucible. The crucible was set in a high-frequency melting furnace (Rigaku Cat. No.3091A001), and fused at 1200°C for 450 seconds. The H_2O- in the flux is also released by the heating at 450°C for 4.5 hours before the mixing with the sample powder. The prepared glass bead has a dilution ratio of 2.065, thickness of ca. 5mm, and a diameter of 4.0cm.

Instrumental conditions for the quantitative analysis are shown in table 1. The reason why the Rubidium, Strontium, Yttrium and Zirconium were chosen for the analysis of trace elements is the way of discrimination of obsidian for Mochizuki *et al.* (1994) and Ikeya (2009) is based on the X-ray intensities of Kα and Kβ spectra of these elements. Power voltage and current condition to the X-ray anode are 50kv and 50mA, respectively. Analytical diameter or diaphragm of 3.0cm (maximum) was used for all measurements. Total analytical time is 27.7 minutes. The dispersive crystal of LiF (220) is chosen for the analyses of the Rb-Kα and Zr-Kα lines, while that of LiF (200) is chosen for the analyses of Fe-Kα, Mn-Kα, Sr-Kα and Y-Kα lines. Lattice spacing of the LiF (220) is relatively narrow than that of the LiF (200) expecting relatively higher

Table 2. Results of correlation lines for quantitative analysis

					Overlap			*Standards*	
	Slope	Intercept	*Acc.*	*R*	line	coefficient	*l.l.d.*	*av.*	*diff.%*
SiO_2	4.04400	-2.27246	0.33780	0.99972	-	-	-	62.66	0.54
TiO_2	7.60641	-0.01872	0.00850	0.99988	-	-	0.0000134	0.51	1.66
Al_2O_3	4.22062	-0.23783	0.12517	0.99979	-	-	0.0000578	14.04	0.89
$Fe_2O_3^T$	38.02513	0.02124	0.06669	0.99991	-	-	0.0000042	5.46	1.22
MnO	29.35220	0.02236	0.00154	0.99976	-	-	0.0000018	0.10	1.53
MgO	1.80152	-0.06994	0.05153	0.99999	-	-	0.0000037	5.45	0.95
CaO	24.10841	-0.01677	0.03217	0.99998	-	-	0.0000172	4.90	0.66
Na_2O	0.74633	-0.01297	0.04331	0.99983	-	-	0.0000548	3.04	1.42
K_2O	27.24640	-0.09968	0.03414	0.99995	-	-	0.0000001	3.00	1.14
P_2O_5	10.60418	-0.04850	0.00400	0.98975	-	-	0.0000100	0.08	5.14
Rb	0.00719	0.06538	4.31255	0.99952	-	-	0.0016016	117	3.70
Sr	0.01694	-0.19008	6.64874	0.99915	-	-	0.0056185	189	3.51
Y	0.01562	-0.15629	1.45033	0.99933	Rb-Lα	0.17524	0.0038345	29.3	4.95
Zr	0.00889	-0.42480	5.99593	0.99984	Sr-Lα	0.07017	0.0015983	145	4.14

Acc., Accuracy; *R*, Correlation coefficient; *l.l.d.*, lower limit of detection; *av.*, mean value of standard samples; *diff.%*, 100 × *Acc./av.;* major oxides in *wt.%;* trace elements in *ppm.*

Table 3. Results of quantitative analysis of standard samples and cross check samples

	JB-1b		GSP-2		BHVO-2		AGV-2	
wt.%	*r.v.*	*value*	*r.v.*	*value*	*r.v.*	*value*	*r.v.*	*value*
SiO_2	51.66	52.08	66.60	67.02	49.90	49.64	59.30	59.99
TiO_2	1.27	1.27	0.66	0.68	2.73	2.76	1.05	1.06
Al_2O_3	14.53	14.37	14.90	15.00	13.50	13.35	16.91	17.07
$Fe_2O_3^T$	9.12	9.06	4.90	4.96	12.30	12.29	6.69	6.82
MnO	0.15	0.15	0.04	0.04	0.17	0.17	0.10	0.10
MgO	8.23	8.46	0.96	0.95	7.23	7.22	1.79	1.78
CaO	9.70	9.66	2.10	2.09	11.40	11.38	5.20	5.22
Na_2O	2.66	2.64	2.78	2.77	2.22	2.22	4.19	4.21
K_2O	1.33	1.30	5.38	5.48	0.52	0.52	2.88	2.93
P_2O_5	0.26	0.26	0.29	0.29	0.27	0.26	0.48	0.48
total	98.91	99.24	98.61	99.27	100.24	99.82	98.59	99.65
ppm								
Rb	39.5	35.9	245	253	9.8	7.6	68.6	71.0
Sr	444	458	240	246	389	394	658	669
Y	-	24.4	28.0	29.3	26.0	27.7	20.0	21.1
Zr	-	132	550	564	172	168	230	226

	RGr		RGb		RGbr	
wt.%	*p.v.*	*value*	*p.v.*	*value*	*p.v.*	*value*
SiO_2	71.81	72.37	47.33	46.94	58.27	58.11
TiO_2	0.04	0.04	0.18	0.18	0.11	0.11
Al_2O_3	15.51	15.62	15.83	15.65	15.50	15.47
$Fe_2O_3^T$	2.14	2.16	12.67	12.43	7.84	7.84
MnO	0.19	0.18	0.22	0.22	0.22	0.22
MgO	0.11	0.09	14.78	14.75	7.98	7.97
CaO	2.07	2.06	8.71	8.65	5.40	5.38
Na_2O	3.64	3.61	0.57	0.56	2.01	2.01
K_2O	3.92	3.92	0.10	0.11	2.03	2.03
P_2O_5	0.06	0.06	0.02	0.02	0.05	0.04
total	99.49	100.13	100.39	99.50	99.41	99.19
ppm						
Rb	72.8	72.8	3.1	3.5	37.8	39.7
Sr	270	267	403	407	333	342
Y	98.8	98.1	4.1	4.2	60.1	61.3
Zr	251	239	17.8	19.2	131	134

value, results in this study; *r.v.,* recommended values of standard samples; *p.v.,* preferable values of cross check samples; *Acc.,* Accuracy; *R,* Correlation coefficient; Total Fe as Fe_2O_3.

peak/background ratio (i.e. S/N ratio) and resolution, whereas requiring relatively longer analytical time for keeping the same accuracy.

Results of constant numbers of the calibration lines for the analysis elements are shown in table 2. Coefficient values for the correction of matrix effect were calculated on the basis of Fundamental Parameter (FP) method, in which the de Jongh model (i.e. self-absorption model) was chosen for calculation, and the Ig (ignition loss) was regarded as base. This calculation was carried out using the PC program equipped with the ZSX PrimusIII+. Coefficient values for the correction of overlap spectra on analysis lines, Rb-Lα spectrum on Y-Kα line, and Sr-Lα spectrum on Zr-Kα line, were also calculated using the PC program equipped with the ZSX PrimusIII+. In addition to these, corrections of the absorption effects by the flux, ignition loss, gain on ignition, and dilution rate in the glass beads were also taken into account for the calculations. The results of constructed calibration lines indicate that the correlation coefficient values are more than 0.999, and accuracy are less than 5.2% in all elements.

2-2 Propriety of instrumental conditions

Geochemical standard samples of GSJ (JB-1b) and USGS (GSP-2, BHVO-2 and AGV-2) were analyzed to check the propriety of the analytical method. Further-

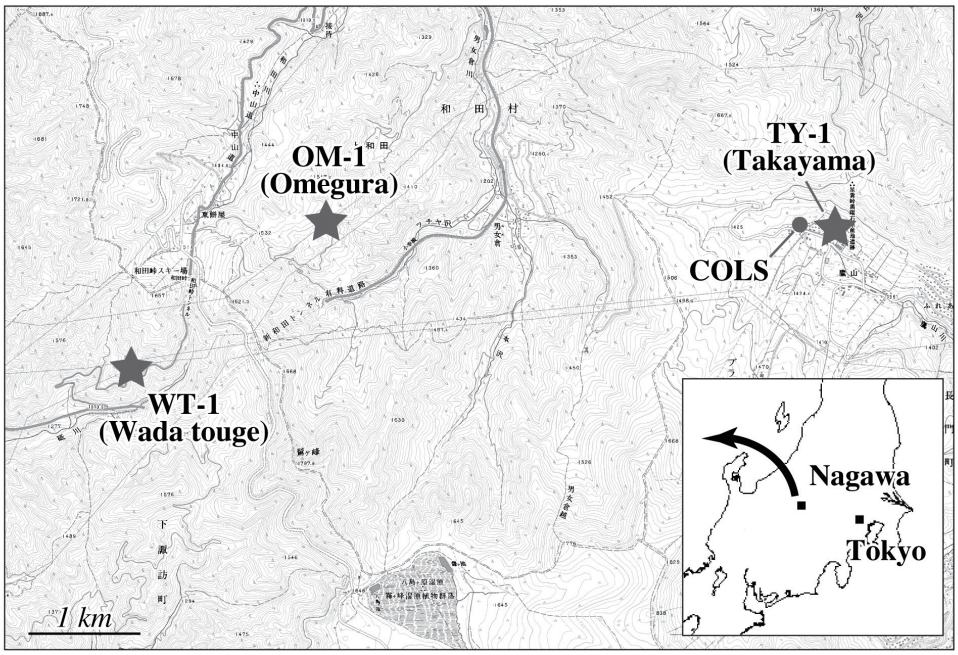

Fig. 1 Localities of obsidian analyzed in this study, and Meiji University Center for Obsidian and Lithic Studies (COLS) in Nagawa town area. Index map showing locality of Nagawa town in Japan.

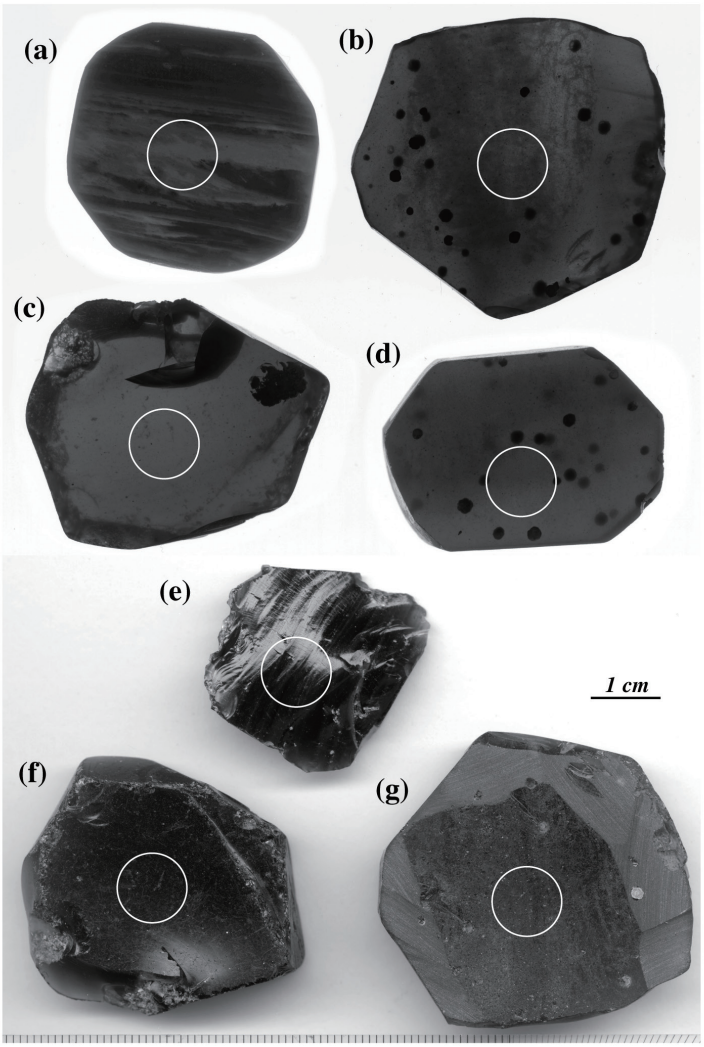

Fig. 2 Photographs showing polished slab surface (a-d), flaked surface (e), weathered surface (f, g) of analyzed obsidian from Wada touge (WT-1; a, e), Omegura (OM-1; b, d, g), and Takayama (TY-1; c, f). Circles indicate analytical points by WDXRF.

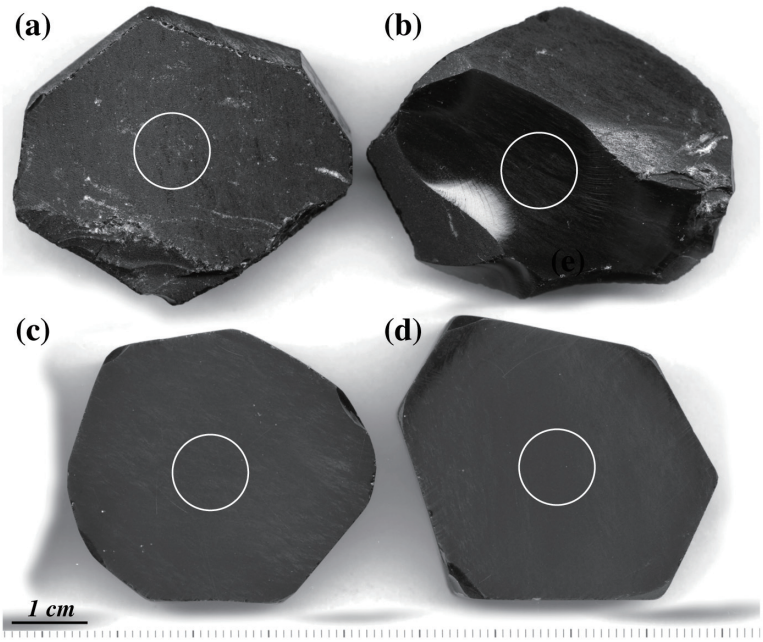

Fig. 3 Photographs showing weathered surface (a), flaked surface (b), and polished sawn surface (c, d) of analyzed obsidian from Shirataki (obstd-1). Circles indicate analytical points by WDXRF.

more, samples of RGr, RGbr and RGb reported in Suda *et al.* (2010; 2011), and Suda and Motoyoshi (2011) were also analyzed for cross checking purpose. The results of analysis are shown in table 3. The analysis was repeated three times for each sample. The values were estimated from the average of all the analyses. The results indicate that the difference between the analytical values and the recommended or preferable values is generally less than 5%. Largest difference is shown in the Rubidium content of the BHVO-2, where the difference reaches up to 26%.

2-3 Analysis of obsidian

2-3-1 Sample description and preparation

Analyses of geological obsidian from Shirataki (obstd-1), Takayama (TY-1), Omegura (OM-1) and Wada touge (WT-1) were performed. Locality of the samples excluding the Shirataki is shown in fig. 1. Appearances of the analyzed samples are shown in figs. 2 and 3. Only the locality of obsidian from Shirataki is not exactly known, which could be derived from Shirataki in Hokkaido, and has been displayed in the entrance of COLS building as a monument. Therefore, this obsidian is called obstd-1 in this study. The appearance of the obstd-1 is characterized by homogeneous black-colored glass without any inclusion, such as fragments of rocks, and bubbles formed by a sparkling of magmatic gas. On the other hand, the TY-1, and OM-1 contain some small inclusions, and the WT-1 has typical foliated texture.

Sample preparation for analysis was carried out by the following manner. 1) Sample was cut using a diamond saw, and a slab with a thickness of ca. 1.0cm, and the diameter of lass than 5cm was prepared. 2) Put the slab into the jaw crusher, and make them into small fragments with one or two millimeters in size. 3) Pick the fragments without any alteration and inclusions up 10g to 20g. 4) Put the fragments into the ultra-deionized water (Millipore Direct-Q UV), and wash them using the ultrasonic cleaning machine until the water becomes completely clear. 5) Dry the fragments using an oven at 110°C for more than 2 hours. 6) Make the fragments into powder using a steel mortar, and an agate mortar. 7) The powdered samples are again heated using a dry oven at 110°C for more than 6 hours until the H_2O^- will be completely excluded. 8) Put the powder into the glass bottle, and keep them in a desiccator. Condition of humidity is kept at less than 30%.

2-3-2 Results

Results of quantitative analysis are shown in table 4. The values of obstd-1 were estimated on the basis of the analysis using five fused glass beads. The analysis was repeated three-times in each glass bead (i.e. total

Table 4. Results of quantitative analysis of obsidian

	obstd -1-2	obstd -1-3	obstd -1-4	obstd -1-5	obstd -1-6	obstd-1-whole (Shirataki)				
wt.%	*value*	*value*	*value*	*value*	*value*	*a.v.*	-	+	*s.d.*	*c.v. %*
SiO_2	76.50	77.11	77.16	77.24	77.95	77.19	76.44	78.03	0.4827	0.63
TiO_2	0.04	0.04	0.04	0.04	0.04	0.04	0.04	0.04	0.0005	1.27
Al_2O_3	12.83	12.95	12.97	12.99	13.12	12.97	12.82	13.13	0.0978	0.75
$Fe_2O_3^T$	1.47	1.47	1.47	1.46	1.47	1.47	1.46	1.48	0.0040	0.27
MnO	0.05	0.05	0.05	0.05	0.05	0.05	0.05	0.05	0.0000	0.00
MgO	0.01	0.01	0.01	0.01	0.02	0.01	0.01	0.02	0.0019	14.35
CaO	0.53	0.53	0.53	0.53	0.54	0.53	0.53	0.54	0.0024	0.45
Na_2O	3.90	3.91	3.91	3.91	3.91	3.91	3.87	3.92	0.0111	0.28
K_2O	4.57	4.56	4.57	4.57	4.58	4.57	4.56	4.58	0.0063	0.14
P_2O_5	0.02	0.02	0.02	0.02	0.02	0.02	0.02	0.02	0.0004	1.99
total	99.92	100.66	100.74	100.83	101.70	100.77	99.82	101.80		
ppm										
Rb	155	151	151	150	145	151	144	158	3.8	2.5
Sr	30.1	29.6	29.4	29.2	28.1	29.3	28.0	30.2	0.7	2.5
Y	28.7	27.5	27.6	27.4	25.9	27.4	25.6	28.9	0.9	3.5
Zr	70.1	67.3	67.3	66.9	63.7	67.0	63.6	70.7	2.1	3.1

	TY-1 (Takayama)			OM-1 (Omegura)			WT-1 (Wada touge)		
wt.%	*value*	-	+	*value*	-	+	*value*	-	+
SiO_2	77.09	76.71	77.52	76.99	76.72	77.57	76.51	76.28	76.62
TiO_2	0.07	0.07	0.07	0.08	0.08	0.09	0.06	0.06	0.06
Al_2O_3	12.70	12.62	12.77	12.69	12.66	12.79	12.69	12.65	12.71
$Fe_2O_3^T$	0.97	0.97	0.97	1.05	1.04	1.05	0.95	0.95	0.95
MnO	0.10	0.10	0.10	0.09	0.09	0.09	0.11	0.11	0.11
MgO	0.02	0.02	0.03	0.03	0.03	0.03	0.02	0.01	0.02
CaO	0.49	0.49	0.49	0.54	0.53	0.54	0.50	0.50	0.50
Na_2O	3.98	3.96	4.01	3.97	3.92	3.99	4.08	4.06	4.10
K_2O	4.73	4.73	4.74	4.73	4.73	4.74	4.56	4.55	4.58
P_2O_5	0.01	0.01	0.01	0.01	0.01	0.01	0.01	0.01	0.01
total	100.17	99.65	100.71	100.19	99.80	100.91	99.48	99.18	99.66
ppm									
Rb	271	264	279	256	248	261	325	320	332
Sr	8.6	8.2	9.0	13.9	13.4	14.0	8.2	8.0	8.4
Y	44.4	43.2	45.7	37.5	35.9	38.4	50.7	49.9	51.8
Zr	87.4	84.9	89.6	92.5	89.1	94.0	90.2	89.4	91.8

s.d., standard deviation (σ); *c.v.,* coefficient of variation (%); Total Fe as Fe_2O_3.

fifteen times of analysis). The values of TY-1, OM-1 and WT-1 were estimated on the basis of the analysis using the two glass beads. The analysis was repeated three times in each glass bead (i.e. total six times of analysis in each sample).

Results of the analysis are compiled in the multi-element spiderdiagram to evaluate the geochemical characteristics of the obsidian (fig. 4a). All of the values are normalized by the recommended values of JR-1. The compositions of the JR-2 are shown for comparison. The JR-1 and JR-2 are the geochemical standard reference samples of GSJ (Imai *et al.* 1995), which are made from the obsidian in the north of Wada touge (Wada-N) and south of Wada touge (Wada-S), respectively. This diagram indicates that the profiles of TY-1, OM-1, WT-1, and JR-2 are generally similar, but completely differed from the profile of obstd-1.

Geochemical characteristics of TY-1, OM-1 and WT-1 are examined more precisely on the spiderdiagram for selected elements (fig. 4b). Although the patterns of TY-1, OM-1 and WT-1 generally have similar profiles, the ratio of normalized values between Rb_N and Sr_N, and Sr_N and Y_N are slightly differed among the patterns. This suggests that geochemistry of the obsidian can be characterized on the basis of the Rb/Sr ratio and the Sr/Y ratio.

The JR-1 normalized variation diagram of Sr/Rb ratio versus Y/Sr ratio is shown in fig. 5, in which mineral vectors indicating a compositional trend by the fractional crystallization of indicated minerals are

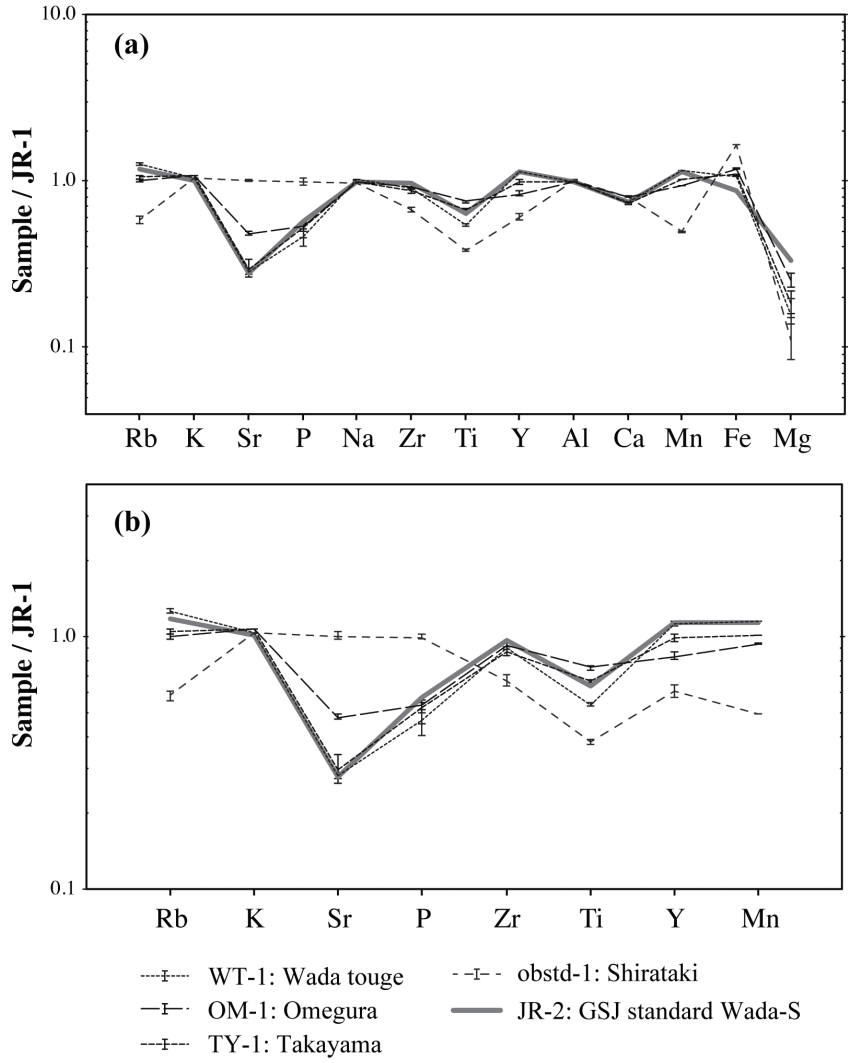

Fig. 4 JR-1 normalized multi-element (a) and selective multi-element (b) spiderdiagrams for obsidian.

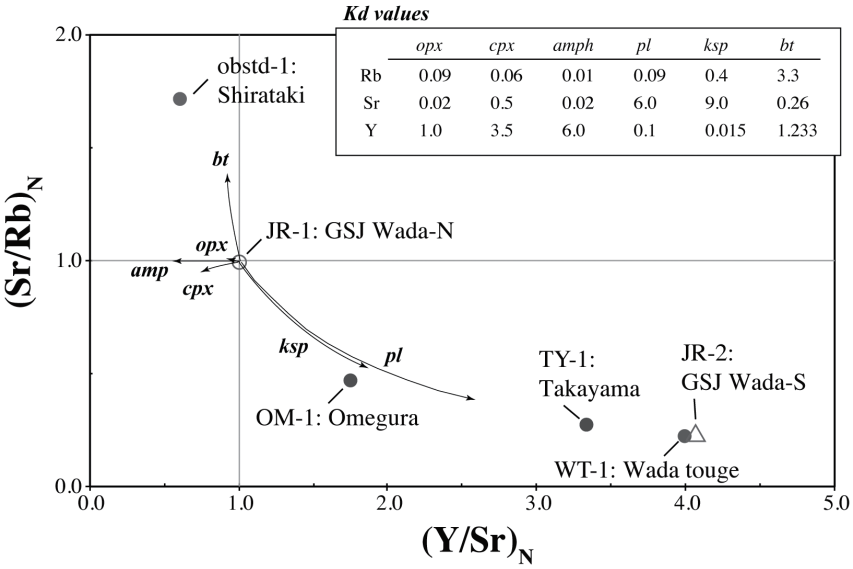

Fig. 5 Variation of JR-1 normalized Sr/Rb ratio versus Y/Sr ratio for obsidian. Mineral vectors calculated from the partition coefficient (***Kd***) values (index) are also compiled. Mineral abbreviations: ***pl,*** plagioclase; ***ksp,*** K-feldspar; ***cpx,*** clinopyroxene; ***opx,*** orthopyroxene; ***amp,*** amphibole; ***bt,*** biotite.

also shown for comparison. Partition coefficient values between minerals and rhyolitic liquid indicate that the Rubidium is compatible with biotite (Henderson and Henderson 2009). Strontium is compatible with feldspars, while incompatible with the mafic minerals (e.g. clinopyroxene, amphibole and biotite). Yttrium is compatible with the mafic minerals, while incompatible with the feldspars. Namely, abundance of these elements is related with the fractional crystallization process of the minerals. Moreover, following the Rayleigh fractional crystallization model, the Sr/Rb ratio decreases by the fractional crystallization of feldspars, while increases by the fractional crystallization of mafic minerals. On the other hand, the Y/Sr ratio increases by the fractional crystallization of feldspars, while decrease by the fractional crystallization of mafic minerals.

On the variation diagram shown in fig.5, the JR-1 is plotted in the point across the lines of x=1.0 and y=1.0. The obstd-1 is plotted in the field of higher Sr/Rb ratio and lower Y/Sr ratio. The TY-1, OM-1 and WT-1 are plotted in the field completely away from the points of obstd-1 and JR-1, in which the TY-1, OM-1 and WT-1 are plotted in the field of lower Sr/Rb ratio and middle to higher Y/Sr ratio. The WT-1 is almost overlapped with the point of JR-2. The composition of TY-1, OM-1 and WT-1+JR-2 are distinguishable using the value of Y/Sr ratio, in which the WT-1+JR-2 has the highest Y/Sr ratio, the OM-1 has the lowest Y/Sr ratio, and the TY-1 has the median Y/Sr ratio. Alignment of the points from JR-1 through OM-1 and TY-1 to WT-1+JR-2 is generally correlated with the mineral vectors indicating the fractional crystallization of feldspars (i.e. *ksp* and *pl*). Namely, compositional variation of the obsidians could be related with the fractional crystallization process of feldspars. Needless to say, although there is a possibility that this compositional variation reflects the diversity of magma source composition, the results clearly indicate that the variation of Sr/Rb ratio versus Y/Sr ratio could become a good indicator to distinguish or characterize the geochemistry of the obsidians.

3. Examination of nondestructive analysis

3-1 Instrumental conditions

Nondestructive analysis of obsidian is still required in many cases of archeological research work, which could be a critical reason to have been unable to perform the quantitative analysis of archeological obsidian. To establish the nondestructive analysis, analysis using the polished slab surface was performed. Subsequently, analysis using the fractured or flacked and weathered surfaces was performed. Finally, the way of data expression will be proposed to link the results of nondestructive analysis with those of quantitative analysis.

All analyzed obsidian slabs have a thickness of ca. 1.0cm, which had been cut by a diamond saw, and pol-

Table 5. Instrumental conditions for analysis of polished, flaked and weathered surfaces of obsidian

Application name:	RockWS4.2	Diaphragm:	10 mm
		Spin:	On

	Line		Target	kV	mA	Filter	Slit	Crystal	Detector	Count time (s)				Angle (deg)		
										Peak	BG1	BG2	total	Peak	BG1	BG2
14	Si	Kα	Rh	50	50	out	S4	PET	PC	80	-	-	80	109.062	-	-
22	Ti	Kα	Rh	50	50	out	S2	LiF(200)	SC	80	40	40	160	86.132	84.662	86.830
13	Al	Kα	Rh	50	50	out	S4	PET	PC	80	40	40	160	144.798	140.650	147.480
26	Fe	Kα	Rh	50	50	out	S2	LiF(200)	SC	80	80	-	160	57.502	55.744	-
25	Mn	Kα	Rh	50	50	out	S2	LiF(200)	SC	80	40	40	160	62.956	62.482	63.420
12	Mg	Kα	Rh	50	50	out	S4	RX25	PC	80	40	40	160	37.968	35.170	40.330
20	Ca	Kα	Rh	50	50	out	S4	LiF(200)	PC	80	40	40	160	113.090	110.650	114.880
11	Na	Kα	Rh	50	50	out	S4	RX25	PC	80	40	40	160	46.128	43.960	47.940
19	K	Kα	Rh	50	50	out	S4	LiF(200)	PC	80	40	40	160	136.662	133.190	139.550
15	P	Kα	Rh	50	50	out	S4	Ge	PC	80	40	40	160	141.110	137.722	142.888
37	Rb	Kα	Rh	50	50	out	S2	LiF(200)	SC	200	100	100	400	26.590	25.982	27.086
38	Sr	Kα	Rh	50	50	out	S2	LiF(200)	SC	200	100	100	400	25.124	24.768	25.516
39	Y	Kα	Rh	50	50	out	S2	LiF(200)	SC	200	100	100	400	23.784	23.414	24.254
40	Zr	Kα	Rh	50	50	out	S2	LiF(200)	SC	200	100	100	400	22.540	22.978	22.122
												total	52.0	min		

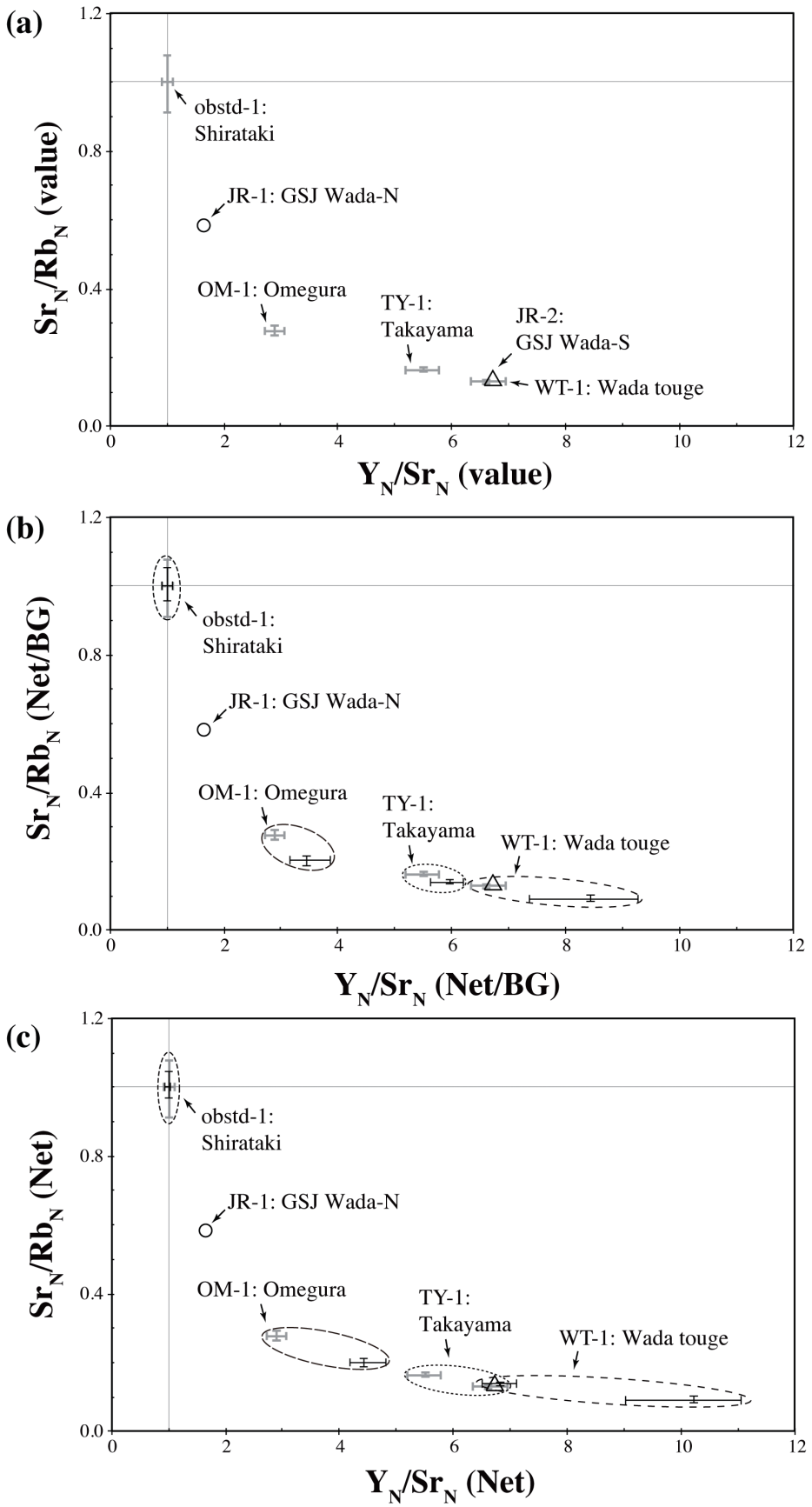

Fig. 6 Variation of obstd-1 normalized Sr/Rb ratio versus Y/Sr ratio for obsidian. Black bars indicating the quantitative value (a), correction X-ray intensity (b), and uncorrected X-ray intensity (c) for analyzed obsidian. Geochemical standard samples of JR-1 (circle) and JR-2 (trigona) (a-c), and quantitative value of analyzed obsidian (gray bars) (b-c) are compiled for comparisons.

ished by diamond paste with 0.3 micron in size (figs. 2 and 3). Instrumental conditions were completely changed from those of the quantitative analysis (table 1), which is shown in table 5. Especially, the analytical diameter or diaphragm was reduced to 1.0cm to be able to choose the analytical point restricted to a homogenous region, or prevented the analysis of inclusions. Dispersive crystal of the LiF (200) was chosen for all measurements. Total analytical time is 52.0 minutes.

3-2 Corrections of matrix effect and overlap spectrum

Corrections of absorption and excitation effects by matrix elements (i.e. matrix effect), and overlap spectrum on an analysis line are necessary to link the analyzed X-ray intensity with actual abundances of element in a sample. The peak-over-background method proposed by Champion *et al.* (1966) is a method for the correction of matrix effect, which is generally used for an analysis of trace elements (e.g. Murata 1993; Kimura and Yamada 1996; Motoyoshi *et al.* 1996). The peak-over-background method is based on a theory that the effect of matrix elements is almost the same both in the peak angle and the background angle. Thus, the matrix effect on an analyzed line will be diminished to normalize the net intensity (Net) by the background intensity (BG).

The correction of overlap spectrum on an analysis line can be combined with the peak-over-background method. The overlap coefficient values were calculated using the PC program equipped with the PrimusIII+. The analysis line for Yttrium (Y-Kα) is completely overlapped with the Rb-K β spectrum, in which the analyzed Y-K α intensity (Y_{Net}) was corrected using the overlap coefficient values (B_Y) and analyzed Rb-K α intensity (Rb_{Net}) on the basis of the following formula: $Y_{Net}-B_Y \times Rb_{Net}$.

3-3 Results

3-3-1 Polished slab surface

Representative analytical points on polished slab surfaces are shown in figs. 2a-d and 3c-d. Analysis of the obstd-1 was performed using ten surfaces of six slabs, the TY-1 was one polished surface, the OM-1 was two surfaces on two slabs, and the WT-1 was two polished surfaces on one slab. All analyses were performed five-times in each surface.

Variation diagrams of Sr/Rb ratio versus Y/Sr ratio are shown in fig. 6. In these diagrams, the values of analyzed samples are normalized by standard values, and plotted on the basis of quantitative value (Value: fig. 6a), correction X-ray intensity by the peak-over-background method (Net/BG: fig. 6b), and uncorrected X-ray intensity (Net: fig. 6c). The standard values were obtained from the analysis of the obstd-1. Therefore, composition of the obstd-1 is predominantly plotted on the point across the lines between x=1 and y=1 in all diagrams.

The diagrams indicate that the results of correction intensity (Net/BG) of analyzed obsidians are generally comparable with the results of quantitative value (Value), whereas the results of uncorrected intensity of analyzed obsidian (Net) are not completely comparable with the results of quantitative value (Value). Namely, the peak-over-background method is useful to link the analyzed X-ray intensity with the actual abundance of element in these diagrams.

3-3-2 Flaked and weathered surfaces

Analysis of flaked and weathered surface of obsidian was performed on the same method as the analysis of polished slab surface. Appearance and analytical points of the samples are shown in figs. 2e-g, and 3a-b. The samples of flaked surface were made from the obstd-1 and the WT-1, while the samples of weathered surface were made from the obstd-1, TY-1 and OM-1. The analysis was repeated five-times in each surface, and the results were compiled in the variation diagram of Sr/Rb ratio versus Y/Sr ratio (fig. 7). In this diagram, the analyzed X-ray intensities were corrected by the peak-over-background method, and normalized by the X-ray intensities obtained from the analysis of polished surface of obstd-1.

The flaked and weathered surfaces of obstd-1, OM-1 and TY-1 are plotted within the range of the values from the analysis of polished surfaces. This result indicates that the ratio of X-ray intensity between the samples is not significantly affected by the condition of analytical surfaces, although analyzed X-ray intensity will easily be affected by the condition of analytical surface. Exceptionally, only the WT-1 is plotted out of the range of the value from polished surface. Appearance of analytical point indicates that WT-1 is developing typical foliated texture (fig. 2a). Thus, compositional heterogeneity on a macroscopic scale could be suggested.

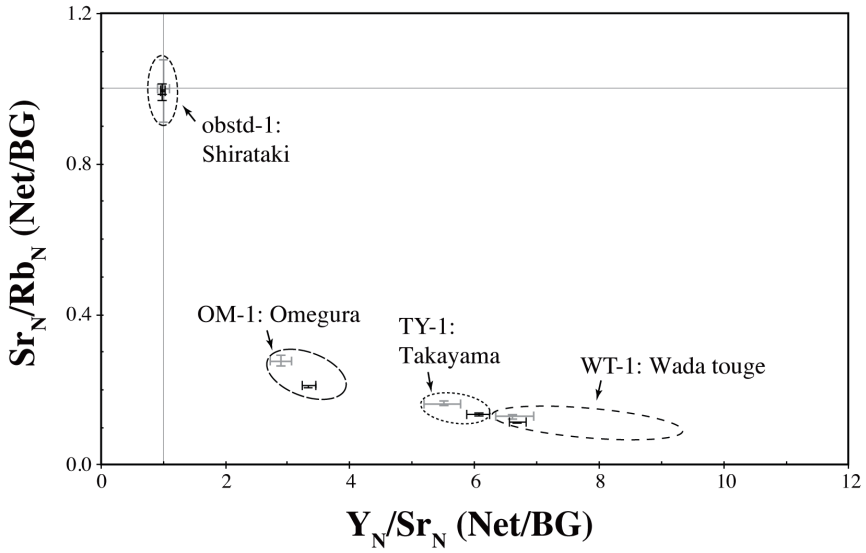

Fig. 7 Variation of obstd-1 normalized Sr/Rb ratio versus Y/Sr ratio for obsidian. Results of analyses by flaked and weathered surfaces of obsidian (black bars), and quantitative value of the obsidian after fig. 6a (gray bars) are compiled. Dashed circles indicating fields of quantitative value, and correction X-ray intensity of obsidian after fig. 6b.

4. Conclusions

4-1 Nondestructive analysis of archeological obsidian artifacts

This study suggests that variation of Sr/Rb ratio and Y/Sr ratio is quite useful to characterize or discriminate the geochemistry of obsidian, which is theoretically supported by the fractional crystallization process of feldspars. Moreover, there are two points to link the results of nondestructive analysis with those of quantitative analysis. One is the X-ray intensity obtained from the nondestructive analysis must be corrected by the peak-over-background method. The other is the results of analysis must be expressed by the values normalized to the values after a standard sample. This method is directly applied to the nondestructive analysis of archeological obsidian artifacts.

4-2 Geochemical standard sample for nondestructive analysis

Establishments of geochemical reference sample (i.e. standard sample) and chemical reference value (i.e. standard value) are necessary to perform the nondestructive analysis of obsidian artifacts. In this study, obstd-1 with polished slab surface was used as the standard sample that was made from the obsidian with homogeneous composition and texture. Although the obstd-1 is an ideal standard sample, a number of standard samples with various compositions are necessary to improve the accuracy of the results of nondestructive analysis. Furthermore, chemical analyses of the standard samples by multiple analytical appliances, such as ICP-MS, INAA etc., are necessary to establish the standard values. If we could accomplish the establishment of the standard samples and the standard values, the nondestructive analysis of archeological obsidian artifacts by the XRFs will be easily performed, and the results of the nondestructive analysis are reasonably shared and verified among researchers.

Acknowledgments

I would like to express my sincerely thanks to Prof. S. Aida, Mr. N. Ohtake and Ms. S. Ohtake to organize the fieldwork and sampling in Nagawa town area. Special thank is extended to Ms. S. Ohtake, who permitted me to use the obsidian displayed in the entrance of the building of COLS. Prof. A. Ono, Mr. J. Hashizume, and Mr. M. Nagai gave me effective comments as for the analyses of archeological obsidian. Manuscript was improved and revised by Dr. S. Kakubuchi at Saga University, and Dr. M. Satish-Kumar at Shizuoka University. This study was supported by the Grants-in-Aid from the Educational and Research Promotion Foundation of Meiji University, and a grant of Strategic Research Foundation Grant-aided Project for Private Universities from Ministry of Education, Culture, Sport, Science, and Technology, Japan (MEXT), 2011-2016 (S1101020).

References

Chanpion, K. P., Taylor, J. C. and Whittem, R. N., 1966, Rapid X-Ray Fluorescence Determination of Traces of Strontium in Samples of Biological and Geological Origin. *Analytical Chemistry,* 38, pp.109-112.

Henderson, P. and Henderson, G. M., 2009, Earth Science data. Cambridge, 277p.

Ikeya, N., 2009, Kokuyouseki Koukogaku. Shinsensha, 306p (in Japanese).

Imai, N., Terashima, S., Itoh, S. and Ando, A., 1995, 1994 complilation values for GSJ reference samples, "Igneous rock series". *Geochemical Journal,* 29, pp.91-95.

Kimura, J. and Yamada, Y., 1996, Evaluation of major and trace element XRF analyses using a flux to sample ratio of two to one glass beads. *Journal of Mineralogy, Petrology and Economic Geology,* 91, pp.62-72.

Kuzmin, Y. V., 2011, The patterns of obsidian exploitation in the late Upper Pleistocene of the Russian Far East and neighbouring Northeast Asia. *National Resource Enviroment and Humans,* 1, pp.67-82.

Mochizuki, A., Ikeya, N., Kobayashi, K. Mutou, Y., 1994, Isekinai ni okeru Kokuyousekisei sekki no gensanchi betu bunpu nitsuite –Numazushi Doteue iseki BBVsou no gensanchi suitei kara–. *Shizuokaken Koukogaku kenkyu,* 26, pp.1-24 (in Japanese).

Motoyoshi, Y., Ishizuka, H. and Shiraishi, K., 1996, Quantitative chemical analyses of Rocks with X-ray Fluorescence Analyzer: (2) Trace elements. *Antarctic Record,* 40, pp.53-63 (in Japanese with English abstract).

Murata, M., 1993, Major and trace elements analysis of Korea Institute of Energy and Resources igneous rock reference samples using X-ray fluorescence spectrometer. *Journal of Naruto College Education.* 8, pp.34-50 (in Japanese with English abstract).

Shackley, M. S., 2011, X-ray fluorescence Spectrometry (XRF) in Geoarcheology. Springer, 231p.

Suda, Y. and Motoyoshi, Y., 2011, X-ray Fluorescence (XRF) Analysis of Major, Trace and Rare Earth Elements for Silicate Rocks by Low Dilution Glass Bead Method. *Antarctic Record,* 55, pp.93-108 (in Japanese with English abstract).

Suda, Y., Okudaira, T. and Furuyama, K., 2010, X-ray fluorescence (XRF; RIX-2100) analysis of major and trace elements for silicate rocks by low dilution glass bead method. *MAGMA,* 92, pp.21-39 (in Japanese).

Suda, Y., Koizumi, N. and Okudaira, T., 2011, X-ray fluorescence analysis of major, trace and rare earth elements for igneous rocks, sedimentary rocks, sediments and soil. *MAGMA,* 93, pp.19-32 (in Japanese).

波長分散型蛍光 X 線分析装置を用いた黒曜石の化学分析

― 考古学的石器石材の非破壊化学分析法の開発 ―

隅　田　祥　光

要　旨

波長分散型とエネルギー分散型（卓上型・携帯型）の各種蛍光 X 線分析装置が明治大学黒耀石研究センター（長野県小県郡長和町）に設置された。これら分析装置を用いた考古学的石器石材の非破壊化学分析法の開発を行った。まず，波長分散型蛍光 X 線分析装置による低希釈ガラスビードを用いた定量分析法の確立を行い，次に，同装置を用いた黒曜石の非破壊分析法について検討した。低希釈ガラスビードを用いた定量分析結果からは，長野県長和町地域における幾つかの黒曜石原産地（男女倉，和田峠，鷹山）の黒曜石試料は，Sr/Rb 比と Y/Sr 比がそれぞれ明瞭に異なり，地球化学的手法によるモデル計算から，マグマからの斜長石の分別結晶作用の程度の違いが反映されているものと示唆された。さらに，非破壊化学分析法の検討からは，Peak-over-background 法による共存元素の吸収励起効果の補正，Y-K α 線に対する Rb-K β のスペクトルの重なり補正を行うことで，標準試料（北海道白滝地域の黒曜石）との相対値として，定量分析値とおおよそ直接的に対比できる結果が得られることが明らかとなった。すなわち，標準試料とその化学分析値を基準とした分析法，解析法は，特に非破壊分析において有効であり，考古学的石器石材の化学分析法へ直接的に適用することができる。

キーワード：黒曜石，蛍光 X 線分析装置，化学分析，地球化学，長和町